JOURNAL OF GEOPHYSICAL RESEARCH, VOL. 114, B01103, doi:10.1029/2007JB005564, 2009

Geodynamic implications for the formation of the Betic-Rif orogen from magnetotelluric studies

A. Martí,[1] P. Queralt,[1] E. Roca,[1] J. Ledo,[1] and J. Galindo-Zaldívar[2,3]

Received 21 December 2007; revised 9 October 2008; accepted 30 October 2008; published 24 January 2009.

[1] Magnetotelluric data from the central Betics mountains (Spain) have been used to determine the electrical resistivity of the crust after a three-dimensional (3D) interpretive approach. At shallow levels (<2 km), the resulting model shows good correlation between the geoelectric structures and the geologic units. At greater depths (>3 km), the most striking and well-resolved feature of the model is an upper-middle crust conductive body, located at the core of the Internal Betics antiform. This approximately 14-km-thick body is interpreted as basic or ultrabasic rocks containing a conducting mineral phase. Its structural location above the sole thrust of the Betic orogen and beneath the Nevado-Filábride complex confirms the presence of a major suture zone between this complex and the autochthonous Iberian plate. This suture may correspond to an ancient oceanic or transitional domain developed between Iberia and the Alboran Domain during the opening of the Tethys Ocean, partially subducted and closed during the development of the Betic orogen. The possible geodynamic scenarios for the Betics have been reconsidered, taking into account this new constraint.

Citation: Martí, A., P. Queralt, E. Roca, J. Ledo, and J. Galindo-Zaldívar (2009), Geodynamic implications for the formation of the Betic-Rif orogen from magnetotelluric studies, *J. Geophys. Res.*, *114*, B01103, doi:10.1029/2007JB005564.

1. Introduction

[2] The magnetotelluric (MT) method utilizes natural electromagnetic energy to characterize the electrical conductivity of the subsurface, being suitable to infer the geoelectrical structures at crustal and lithospheric levels [*Jones*, 1992; *Korja*, 2007]. The main strengths of the MT method are its capability for a broad range of penetration depths, its sensitivity to lateral and vertical electrical conductivity variations and its capability of imaging volumetric structures. In MT, the study depth depends on the period of the electric and magnetic field variations being measured. The relationships between the horizontal components of these fields at a given period are characterized by the impedance tensor (Z), from which components, the apparent resistivity and phase responses, can be computed that are used for analysis and modeling.

[3] Magnetotelluric exploration in orogenic regions has provided valuable information on the structures and processes at depth that can be correlated with other geophysical observations. In the Tibetan-Himalayan orogen [*Unsworth et al.*, 2005], a high-conductivity zone was interpreted as a partially molten layer along the southern margin of the Tibetan plateau. *Wu et al.* [2005] imaged the Proterozoic Wopmay Orogen (Canada), in which a crustal conductor was associated with the collision of two terranes, and a mantle conductor with the presence of graphitic or sulfidic rocks introduced during subduction prior to the collision. Magnetotelluric surveys in the Iapetus Suture Zone (Ireland-Scotland) identified a highly conductive region at middle to lower crustal depths interpreted as sulfide-bearing sediments [*Rao et al.*, 2007]; while other conductive bodies were interpreted as graphite or metallic mineralizations [*Tauber et al.*, 2003].

[4] In the Alpine Belt, magnetotelluric studies of the Cantabrian Mountains (NW Spain) allowed the identification of shallow conductors as foreland basin sediments. Deeper conductors were related to the sole detachment of the mountains and to the presence of faults [*Pous et al.*, 2001]. In the Pyrenees, a lower crustal conductor is identified in the contact zone between the Iberian and European plates, and is interpreted as a zone of partial melting of the subducted Iberian lower crust [*Ledo et al.*, 2000].

[5] The Betic Chain (or Betic Cordillera or Betics), in the western end of the Mediterranean, is a tectonically complex orogen located on the boundary between the Iberian and African plates. On the basis of geological and geophysical data several models have been proposed to explain the geodynamic evolution of the crustal and lithospheric structure of the Betics along with the Rif Mountains and the Alboran Basin. The most widely accepted models include convective removal [*Platt and Vissers*, 1989] or gravitational collapse [*Seber et al.*, 1996] of a thickened lithosphere and rollback subduction of the African slab and subsequent back arc extension [e.g., *Gutscher et al.*, 2002].

[6] With the objective of imaging the Betics crustal structure from a geoelectric point of view, and hence, to

[1] Departament de Geodinàmica i Geofísica, Universitat de Barcelona, Barcelona, Spain.
[2] Departamento de Geodinámica, Universidad de Granada, Granada, Spain.
[3] Instituto Andaluz de Ciencias de la Tierra CSIC, Universidad de Granada, Granada, Spain.

0148-0227/09/2007JB005564$09.00

add and infer new information on its geodynamical processes, a magnetotelluric survey was performed in the central part of the Betic Chain. Data analyses showed the complex dimensionality of the geoelectrical structures [*Martí et al.*, 2004], which lead to modeling the data using a 3D approach. In this paper we present the 3D crustal conductivity model and its interpretation, focusing specifically on a 3D conductor imaged at mid to low crustal depths, and discuss its possible geodynamic implications.

2. Geological and Geophysical Settings

[7] The Betic Chain (Figure 1) lies in the western Mediterranean and its formation initiated during the Late Mesozoic-Cenozoic orogenesis in the far western end of the Alpine-Himalayan belt [*Platt and Vissers*, 1989]. It belongs to the Alboran system that also includes the Alboran Sea and the Rif and Atlas Mountains.

[8] It is generally accepted that the geodynamic evolution of the Betic-Alboran-Rif region includes a stage of subduction and orogenic wedging of the Alboran Domain [e.g., *Doglioni et al.*, 1999; *Jolivet and Faccenna*, 2000], followed by a stage of compression and thrusting along the Gibraltar Arc with coeval extensional opening of the Alboran Basin up to early Miocene times [e.g., *Platt and Vissers*, 1989; *Seber et al.*, 1996; *Gutscher et al.*, 2002]. These events resulted in interesting geological and geophysical records: intermediate and deep seismicity, continental crustal thinning in the Alboran Sea and the Betics, velocity anomalies and lithospheric thinning under the Alboran Sea and High-Middle Atlas.

[9] Within this context, the Betics is divided classically into an External Zone and an Internal Zone (Figure 1). The External Zone outcrops in the northwest and is the Mesozoic cover of the former South Iberian continental margin [*García-Hernández et al.*, 1980]. The Internal Zone, in the southeast, is composed of three main stacked metamorphic complexes, all belonging to the Alboran crustal domain, that were deformed after the compressional orogenic processes of Cretaceous-Paleogene age [*García-Dueñas et al.*, 1992].

[10] The Internal Zone was affected by E-W to ENE-WSW extension in the early–middle Miocene, coeval with compression in the External Zone, leading to crustal thinning of the former Alboran basin and to the formation of N-S to NW-SE compressional structures that produced the main relief of the Betics [*Balanyá and García-Dueñas*, 1987]. In the central part of the chain (Figure 1) the Internal Zone is formed by large E-W Neogene folds that affected the superposed complexes; these are, from bottom to top, the Nevado-Filábride, Alpujárride and Maláguide complexes respectively. At the top of the Alpujárride complex ultramafic rocks outcrop in the Ronda Massif (Ronda peridotites) and are considered to be a segmented slab [*Tubía et al.*, 1997] within this complex. On the other side of Gibraltar Arc, in the Sébtide complex of the Rif Mountains, peridotitic bodies also outcrop in Beni-Bousera [*Reuber et al.*, 1982].

[11] Geophysical data in this zone show its complex crustal structure, e.g., the lack of correlation between the Bouguer anomalies and the highest altitudes (Sierra Nevada and Sierra de los Filabres) [*Torné and Banda*, 1992] and the existence of anomalous velocity zones [*Dañobeitia et al.*, 1998; *Serrano et al.*, 1998]. Seismic reflection profiles [*García-Dueñas et al.*, 1994; *Galindo-Zaldívar et al.*, 1997] do not provide high resolution of structures at depth (lower crust), but do identify horizontal reflectors suggesting the existence of a major upper crust detachment separating the Alboran Domain from the Iberian Massif. Geoelectrically, a conductive lower crustal zone was identified in the Internal Zone, inferred from a two-dimensional (2D) MT survey [*Pous et al.*, 1999].

3. MT Data Acquisition, Analysis, and Modeling

[12] In 2004 we collected broadband MT data in order to provide new information of this area at middle-lower crustal levels. Data were acquired using Metronix ADU-06 systems, with a range of periods from 1 ms to 4000 s. Time series were processed using a robust algorithm [*Egbert and Booker*, 1986], with Remote Reference. The final data set, which included sites acquired in previous surveys, consisted of 45 sites (Figure 1) with medium to high-quality responses.

[13] The dimensionality analysis of the data was performed using the WALDIM algorithm [*Martí et al.*, 2004], based on the invariant parameters of the impedance tensor defined by *Weaver et al.* [2000], and taking into account data errors. The dimensionality results were grouped at each site in period decade bands, where, for the two-dimensional cases, the average strike directions with their error were obtained using random noise generation with variance equal to that estimated for the impedance tensor components (more details in the work of *Martí et al.* [2004]). The results (Figure 2) revealed that the geoelectric structures are mainly 3D, with some 1D cases located over the basins at short periods. Two-dimensional structures with N-S to NNE-SSW and E-W to WNW-ESE orientations were found in the allochthonous zones (Betics), and with E-W to ENE-WSW orientations in the autochthonous zones (Iberian Massif). The more complex dimensionality of the Betic Chain was interpreted as being related to the superimposition of processes that took part in its evolution, whereas the Iberian Massif, only affected by the Variscan deformation, shows a simpler dimensionality. The abundance of 3D structures increases with the period and toward south. Groom and Bailey type decomposition [*Groom and Bailey*, 1989] of the data [*McNeice and Jones*, 2001] corroborates that the data cannot be described as 2D with a prevalent strike direction [*Martí*, 2006]. Consequently, three-dimensional (3D) modeling is mandatory to characterize the electric resistivity of the central Betic crust.

[14] The 3D model mesh consisted of $50 \times 50 \times 25$ elements (270 km (NS) $\times$ 220 km (EW) $\times$ 100 km (depth)). It extended over the central part of the Betics, including the eastern end of the Guadalquivir Basin, the surrounding southern Iberian Massif and a 35-km strip of the Alboran Sea. The initial conductivity distribution was constructed from 1D inversions [*Constable et al.*, 1987] of apparent resistivity and phase obtained from the impedance tensor determinant at each site, and interpolated over the whole model mesh. The tensor determinant represents an average of the components of the impedance tensor and is a rotational invariant, i.e., is independent of the orientation of the measuring axes.

[15] In the Alboran Sea water depth was modeled following the bathymetry, and assigning a resistivity of 0.3 Ω·m to

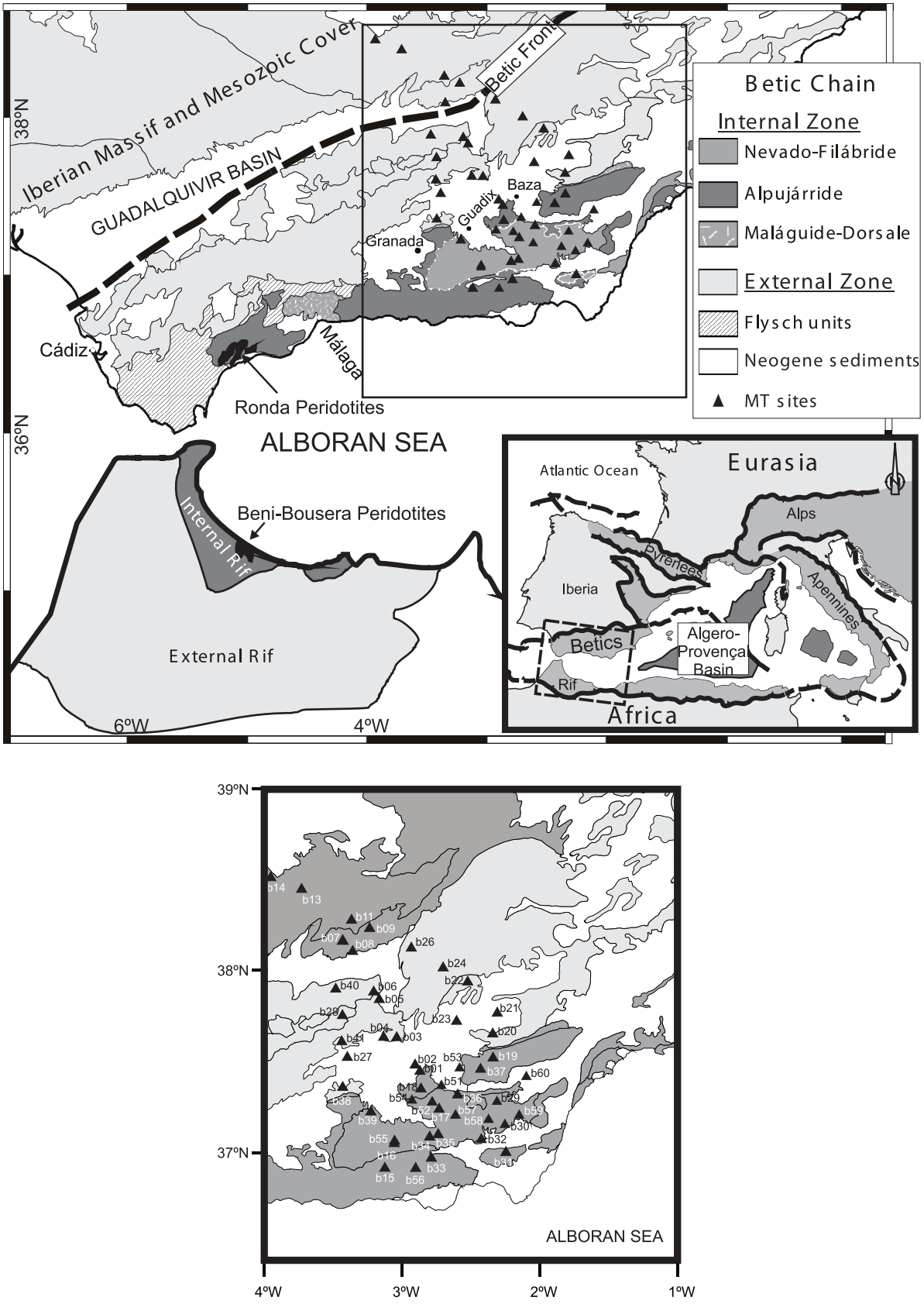

Figure 1. (top) Geological setting of the Betic Cordillera and location of MT sites. (bottom) Padding of the area with MT sites locations with their identification.

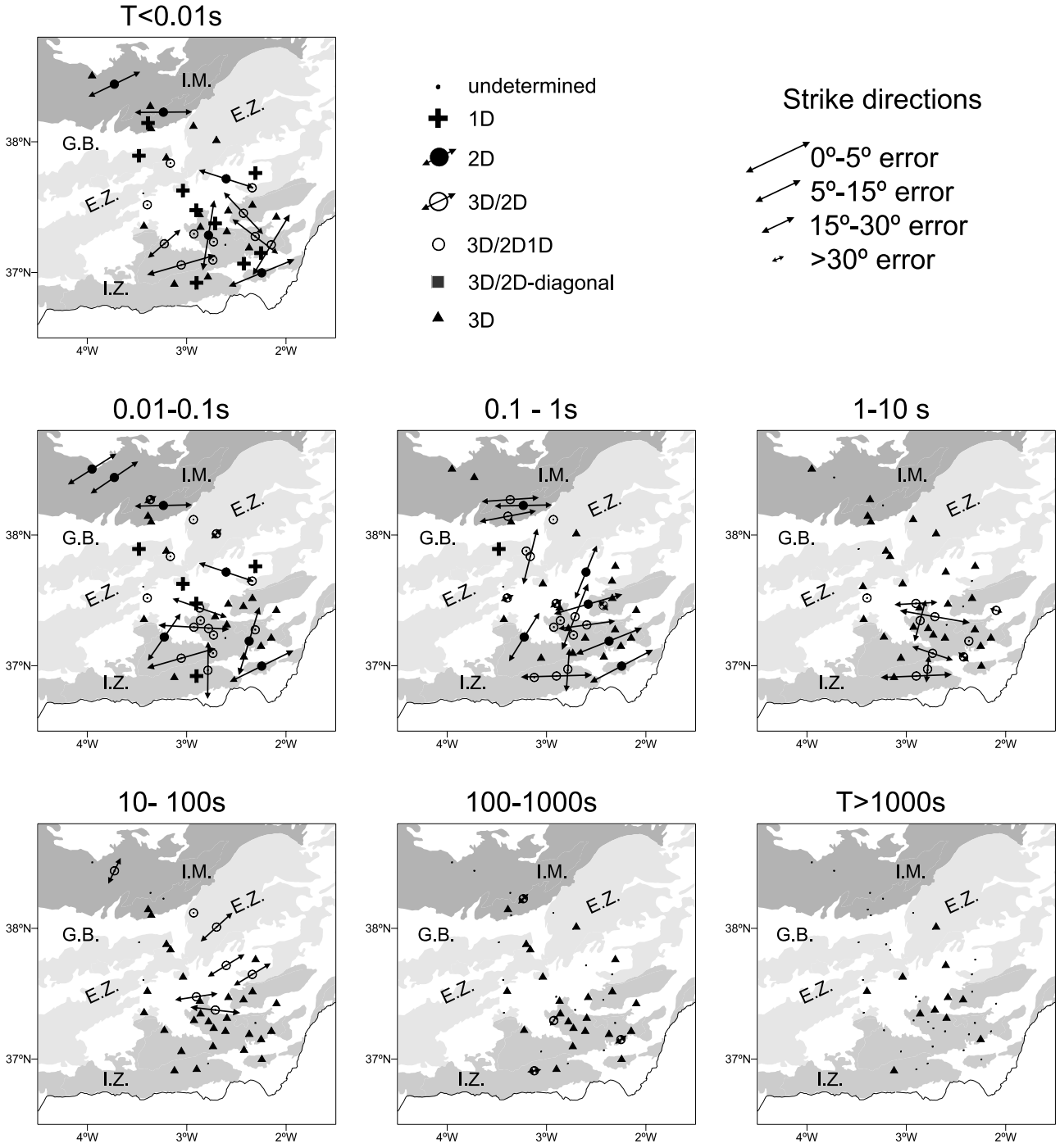

Figure 2. Dimensionality results of the Betics MT data set grouped in 7 period bands. The arrows indicating the strike directions are scaled by the inverse of the error in the determination of the strike. Band 1, $T < 0.01$ s; band 2, 0.01–0.1 s; band 3, 0.1–1 s; band 4, 1–10 s; band 5, 10–100 s; band 6, 100–1000 s; band 7, $T > 1000$ s. I.M., Iberian Massif; G.B., Guadalquivir Basin; E.Z., External Zone; I.Z., Internal Zone.

seawater. At shallow levels this initial model shows a conductivity distribution distinctive for each geological region. In the southeastern part of the model, it shows a high-conductivity structure, at depths greater than 10 km. Three-dimensional forward modeling was undertaken following a trial and error process using the code of *Mackie et al.* [1993] (24 periods, 10^{-3} s to 10^{3} s), fitting the resistivity and phase of the determinant, and, whenever possible, the responses of the off-diagonal components of the impedance tensor. Fitting the determinant is a necessary, but not a sufficient, condition to assure that all components of the impedance tensor are fitted (e.g., *Pedersen and Engels* [2005] proposed this strategy in 2D modeling). It allows obtaining the basic geoelectrical structures, and the model

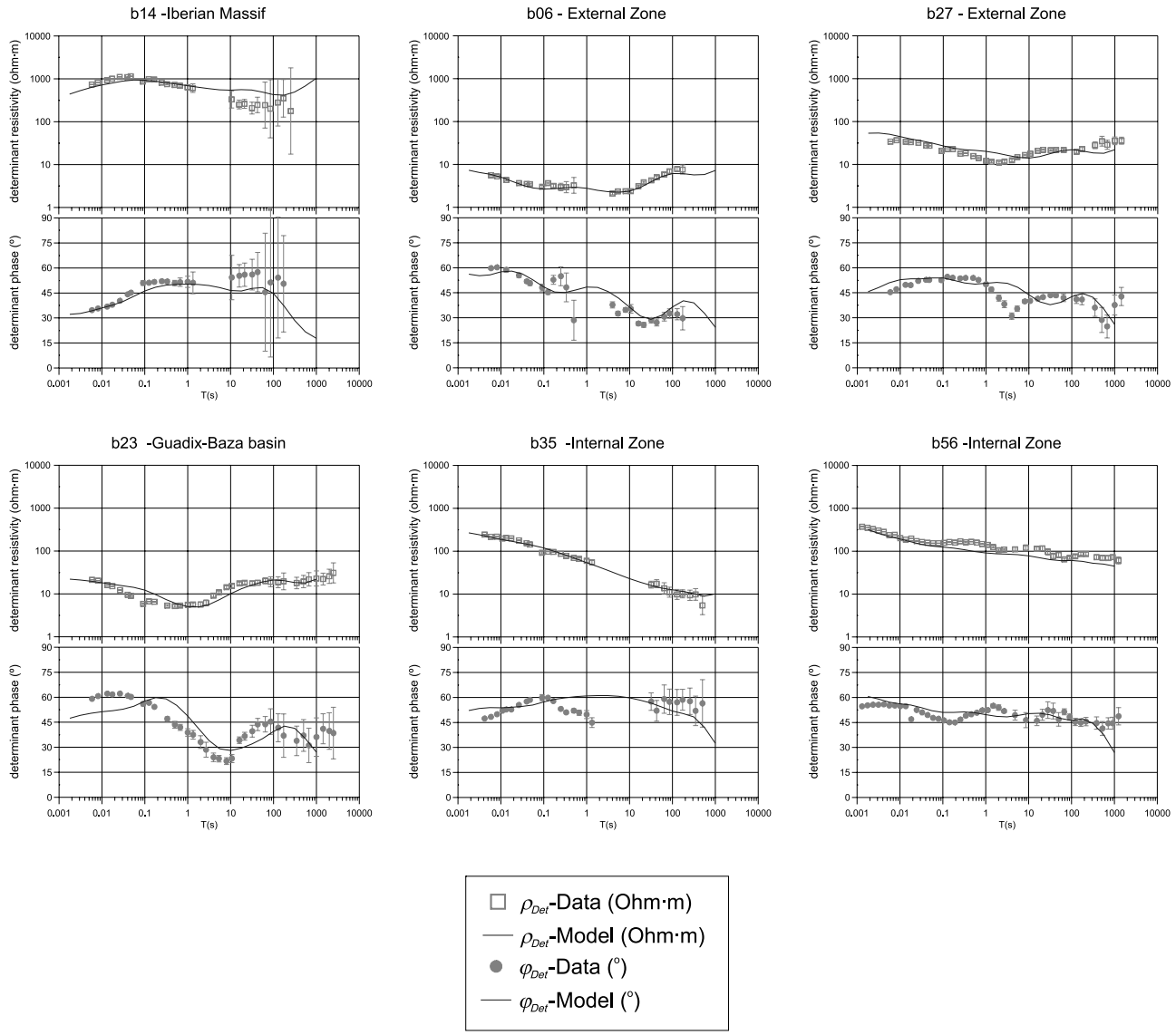

Figure 3a. Determinant data and model responses (resistivity and phase) of six sites, representative of the different geologic zones of the data set: b14 (Iberian Massif), b06 and b27 (External Zone), b23 (Guadix-Baza basin), and b35 and b56 (Internal Zone).

can increase in complexity as more components are fitted. Data and model responses from representative sites are shown in Figure 3, where sites b27 and b23 were rotated to the directions that best fit *xy* and *yx* responses, 45° and −15° respectively. Thus, during the modeling process, the rotation of the data to the quasi-2D coordinate system at these sites, allowed focusing on improving the fit to the off-diagonal elements.

[16] In order to check the stability of the mesh, the model mesh (50 × 50 × 25 elements) was resized to 80 × 80 × 40 elements. Using this new mesh, with the exception of site 14, located at the NW edge of the model, no significant changes in the responses were observed, which confirmed the adequacy of the model mesh used to construct the 3D model. Additionally, sensitivity tests were performed to evaluate the resistivity, depth and extension of the most significant model features (see *Martí* [2006] and next section).

[17] After 140 trials, an acceptable model that fitted the main data trends was obtained. To calculate the RMS values between data and model responses, we used 10% error floor in the resistivities and 2.9° in the phases for the determinant responses, which are standard values useful to avoid overfitting the model when data errors are too large [e.g., *Jones*, 1993; *DeGroot-Hedlin and Constable*, 1993; *Gabàs and Marcuello*, 2003]. The results were RMS(ρ_{DET}) = 4.10 and RMS(φ_{DET}) = 2.32, and for the off-diagonal responses, RMS(ρ_{xy}) = 7.53, RMS(φ_{xy}) = 3.69; RMS(ρ_{yx}) = 11.15 and RMS(φ_{yx}) = 3.99. The RMS values thus obtained can be considered acceptable within the standards [e.g., *Jones et al.*, 2003; *Heise et al.*, 2008].

[18] Maps of determinant RMS at different periods (T = 0.01 s, T = 1 s and T = 100 s) are displayed in Figure 4. In

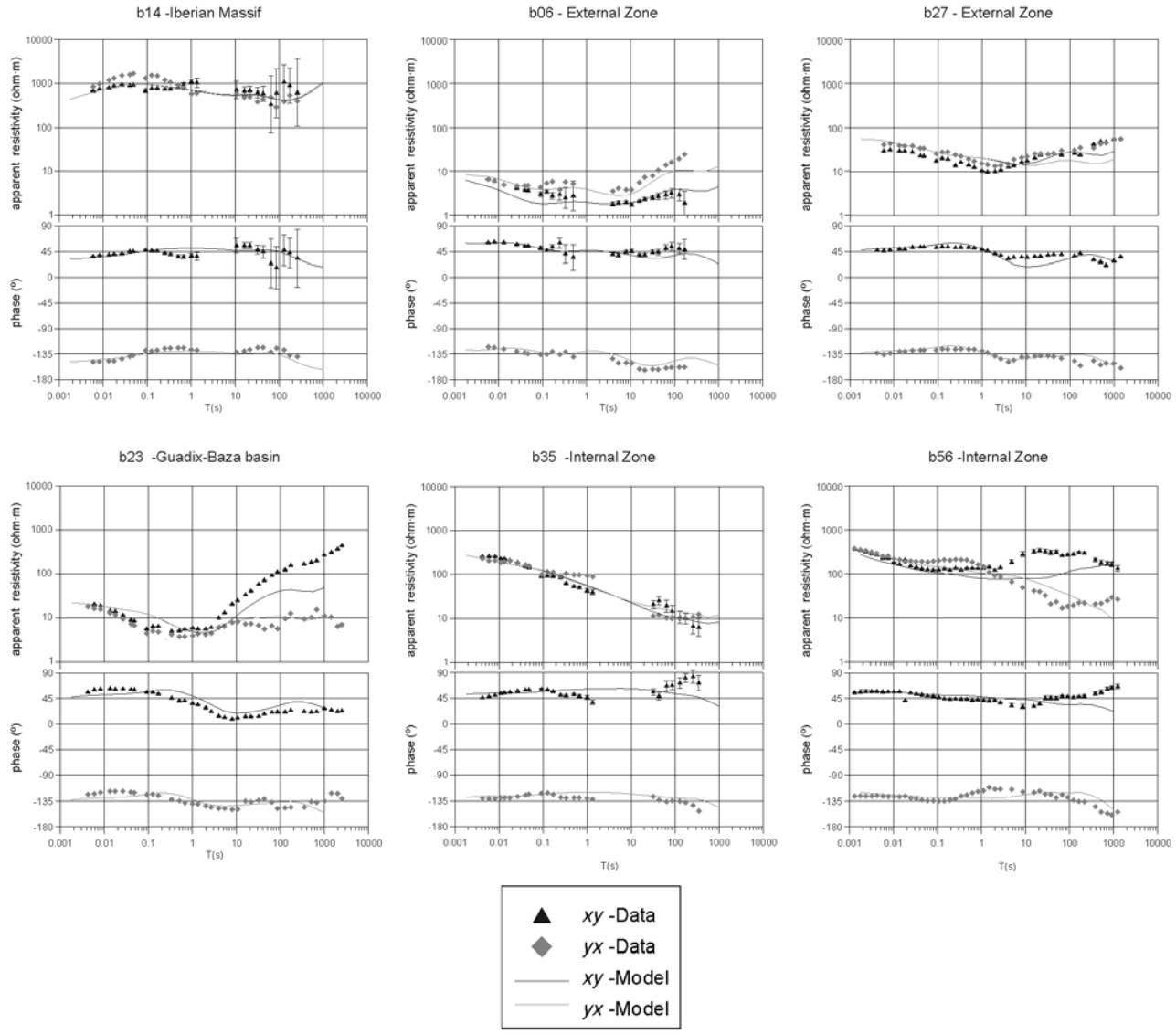

Figure 3b. *xy* and *yx* data and model responses (resistivity and phase) for the same sites. Both *xy* and *yx* data and model responses at sites b27 and b23 have been rotated to the direction of best fit (45° and −15°, respectively).

general, resistivity misfits (RMS(ρ_{DET})) present a broad variation among the different sites and tend to increase with the period, compared to the phase (RMS(φ_{DET})), which have lower and more uniform values. Higher values of RMS(ρ_{DET}) are localized over particular sites of the Internal Betics, and at the NW edge of the model.

4. 3D Electrical Structure and its Interpretation

[19] The model (Figure 5) has a complex resistivity distribution with highly conductive bodies at the uppermost crustal levels (<5 km) in the External Betics and at both the uppermost and middle crustal levels (<17.5 km) in the Internal Betics.

[20] In the Iberian Massif, a resistive zone (**RIM**, Figures 5a–5i) can be associated with metamorphic and granitic rocks. The extension of the resistive zone below the External Zone confirms the continuation of the Iberian basement below the Betics.

[21] A shallow conductor in the Guadalquivir Basin (**CGB**, Figures 5a–5f) is interpreted as water content and fluid circulation in its porous sediments. Its shape shows that the basin infill continues 20–30 km south below the External Zone.

[22] In the External Zone the model shows moderately resistive values at shallow levels, associated with the presence of fluids in the carbonate rocks. Two conductive bodies (**C20** and **C27**–**38,** Figures 5b–5e) are associated with a high content of shales and basaltic rocks and, in the eastern part of this zone, with the presence of flysch rocks.

[23] In the Internal Zone a highly resistive zone (up to 13.5 km) (**RI**, Figures 5a–5g) is interpreted as the presence of metamorphic rocks from the Nevado-Filábride and Alpujárride complexes. Shallow conductors (**C31**, Figures 5c–5d; **CE**, **CF1** and **CF2**, Figure 5e) are interpreted as fluid circulation through superficial faults associated to the detach-

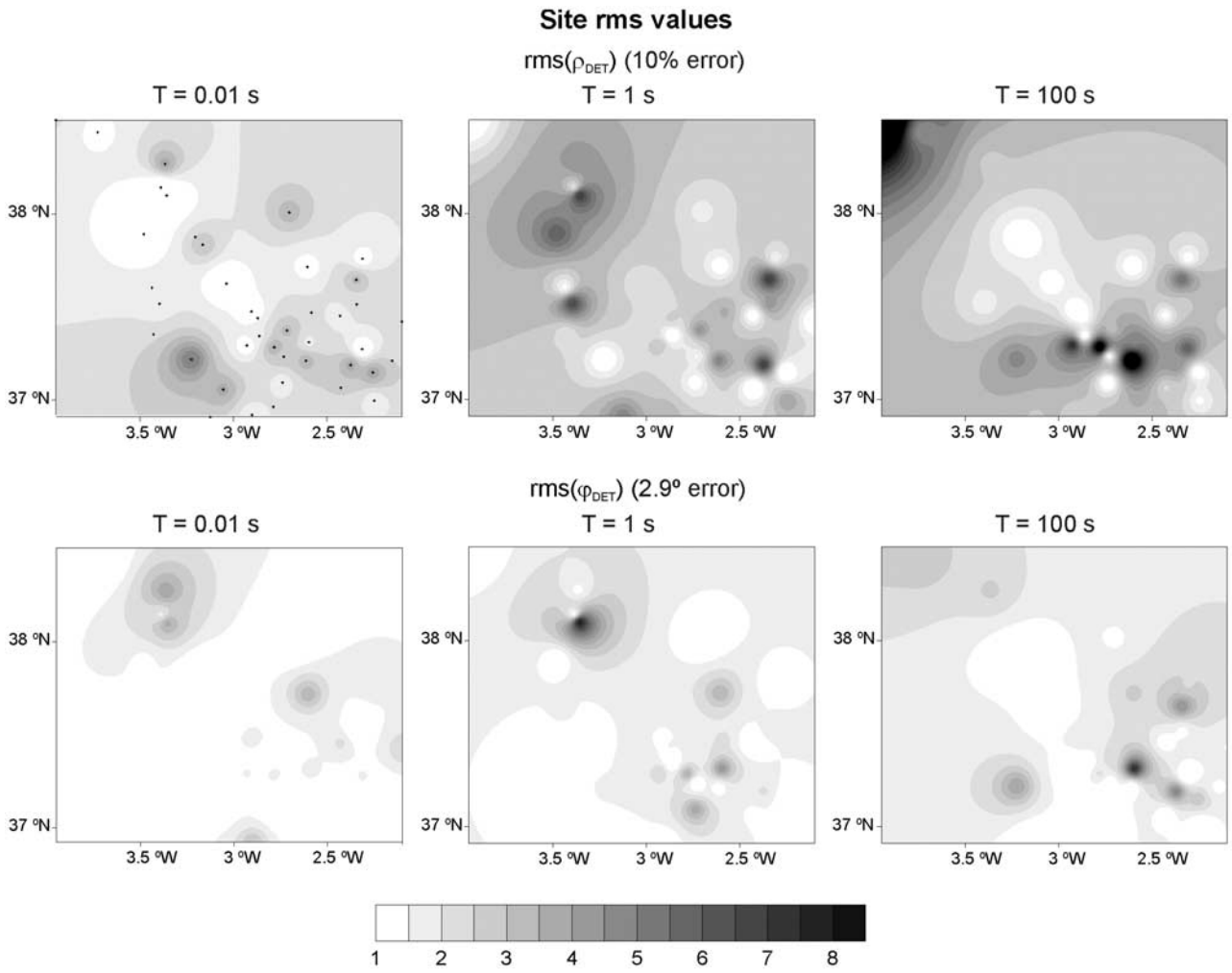

Figure 4. RMS maps of the determinant data and model responses (RMS(ρ_{DET}) and RMS(φ_{DET})) at T = 1 s, T = 10 s, and T = 100 s.

ments bounding the Alpujárride and Nevado-Filábride complexes or different Nevado-Filábride units.

[24] At greater depths the model presents its most remarkable feature: an enigmatic 1 Ω·m to 5 Ω·m conductive body (**CF3**, Figures 5f–5h) located below the main antiform of the Sierra de los Filabres.

[25] To determine the resolution of conductor **CF3**, we performed a sensitivity test, consisting of modifying the resistivity (ρ) and thickness (h) of this body, while keeping the conductance (S = h/ρ) over the area constant. Hence the original 3D model (named bet3d), in which body **CF3** has an average resistivity of 2 Ω·m and a thickness between 3 km (in its westernmost side) and 14 km (in its eastern side), was modified to create two new models. In model bet3d1, both resistivity and thickness were increased by a factor of five to 10 Ω·m and a maximum of 58 km, respectively. In model bet3d2, resistivity was decreased by a factor of five to 0.2 Ω·m and thickness reduced to 3 km (Figure 6). In comparison to the original model bet3d, determinant resistivity RMS values for both models bet3d1 and bet3d2 increased significantly, although phase values remained similar (Table 1). RMS values corresponding to *xy* and *yx* responses increased as well for model bet3d1; while for bet3d2, the model with lower resistivity and thickness, the *xy* responses increased and the *yx* responses decreased. In addition, determinant responses were compared individually for sites located over the center and the edges of the conductor. At site b17, located over the central part of CF3, both resistivity and phase responses corresponding to model bet3d present a better fit to the data than the other two models. For site b57, located over the eastern side of the conductor, model bet3d2 better fits the resistivity responses, but not the phases (Figure 7). A similar behavior can be observed at site b54. On the basis of the resistivity misfits, **CF3** may be more conductive and thinner beneath its edges (sites b57 and b54), although it would not fit the phases. However, according to the overall RMS values (Table 1), the features of **CF3** in bet3d can be considered one reasonable representation of the true 3D distribution of the area.

[26] The presence of a conductive NE-elongated structure below Sierra de los Filabres between 20- and 40-km depth had been proposed using a 2D approach by *Pous et al.* [1999], and was interpreted by those authors as a region of

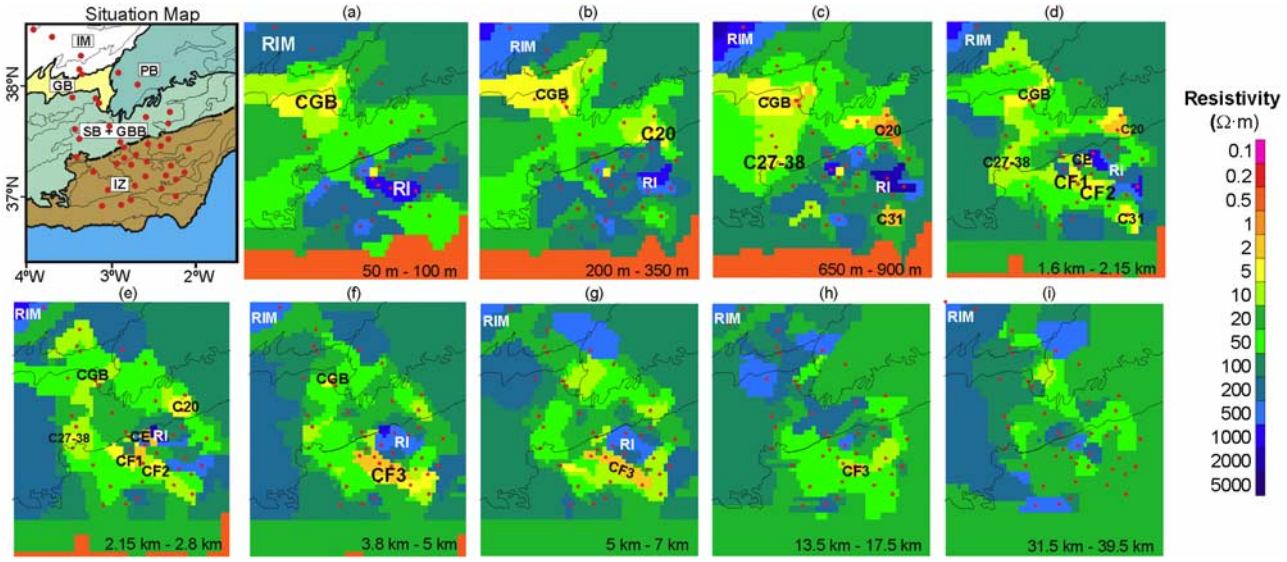

Figure 5. Situation map and horizontal cross sections of the most relevant layers of the 3D model. Situation map: site locations in red; main geologic zones: IM (Iberian Massif), GB (Guadalquivir Basin), PB (Prebetics), SB + GBB (Subbetics + Granada and Guadix-Baza Basin), and IZ (Internal Zone). Cross sections: site locations in red; narrow lines mark the geological divisions; the depth range of each layer is indicated in the bottom right. Abbreviations correspond to the main conductors and resistors described in the text, displayed in a larger font at its upper position. C, conductor; R, resistive. Numbers 20, 27, 31, and 38 refer to sites below which conductors are located.

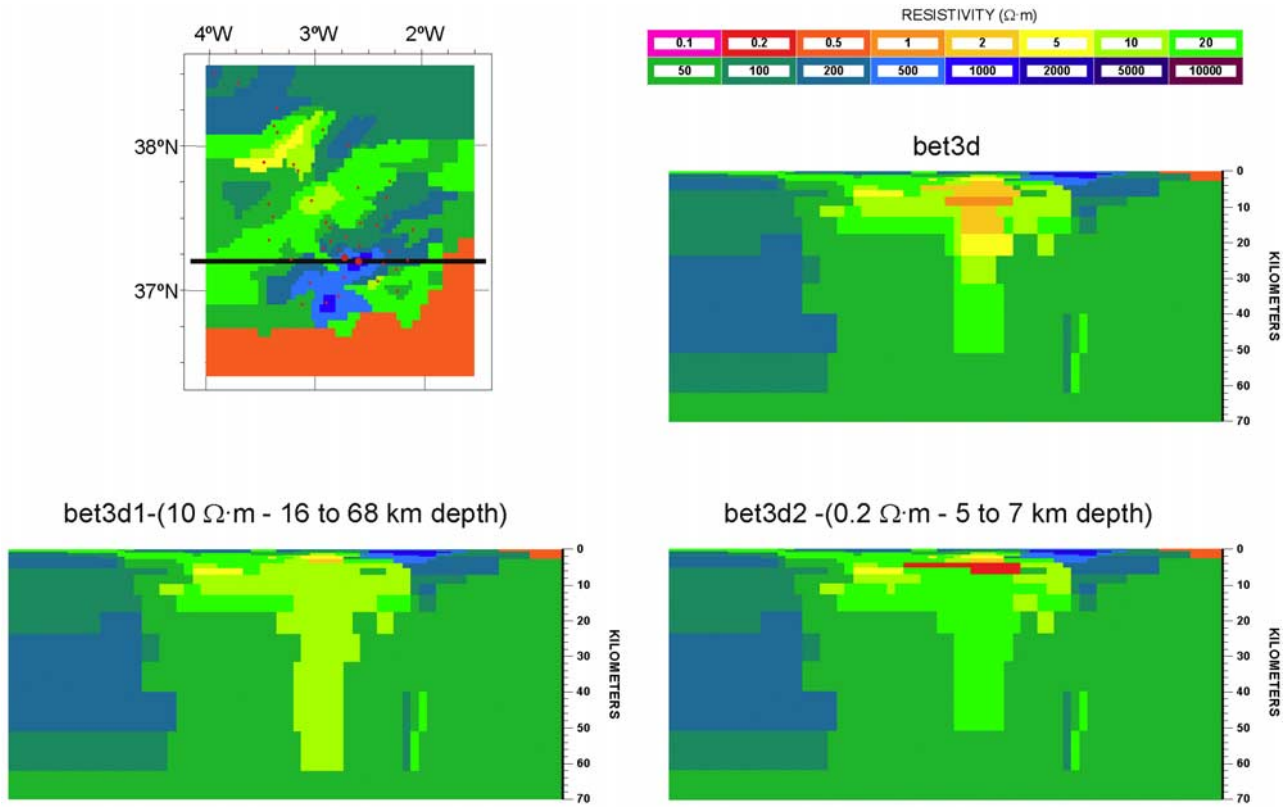

Figure 6. Vertical sections of the models created to test the depth sensitivity of conductor CF3, keeping conductance constant. (top left) Plain view of the 3D model surface with sites and vertical section locations (larger dots indicate, from left to right, sites b17 and b57); (top right) section of model bet3d. (Bottom left) Section of model bet3d1, in which resistivity of CF3 was increased to 10 Ω·m and its depth up to a maximum of 68 km; (bottom right) section of model bet3d2, with resistivity of CF3 decreased to 0.2 Ω·m and a maximum depth of 7 km.

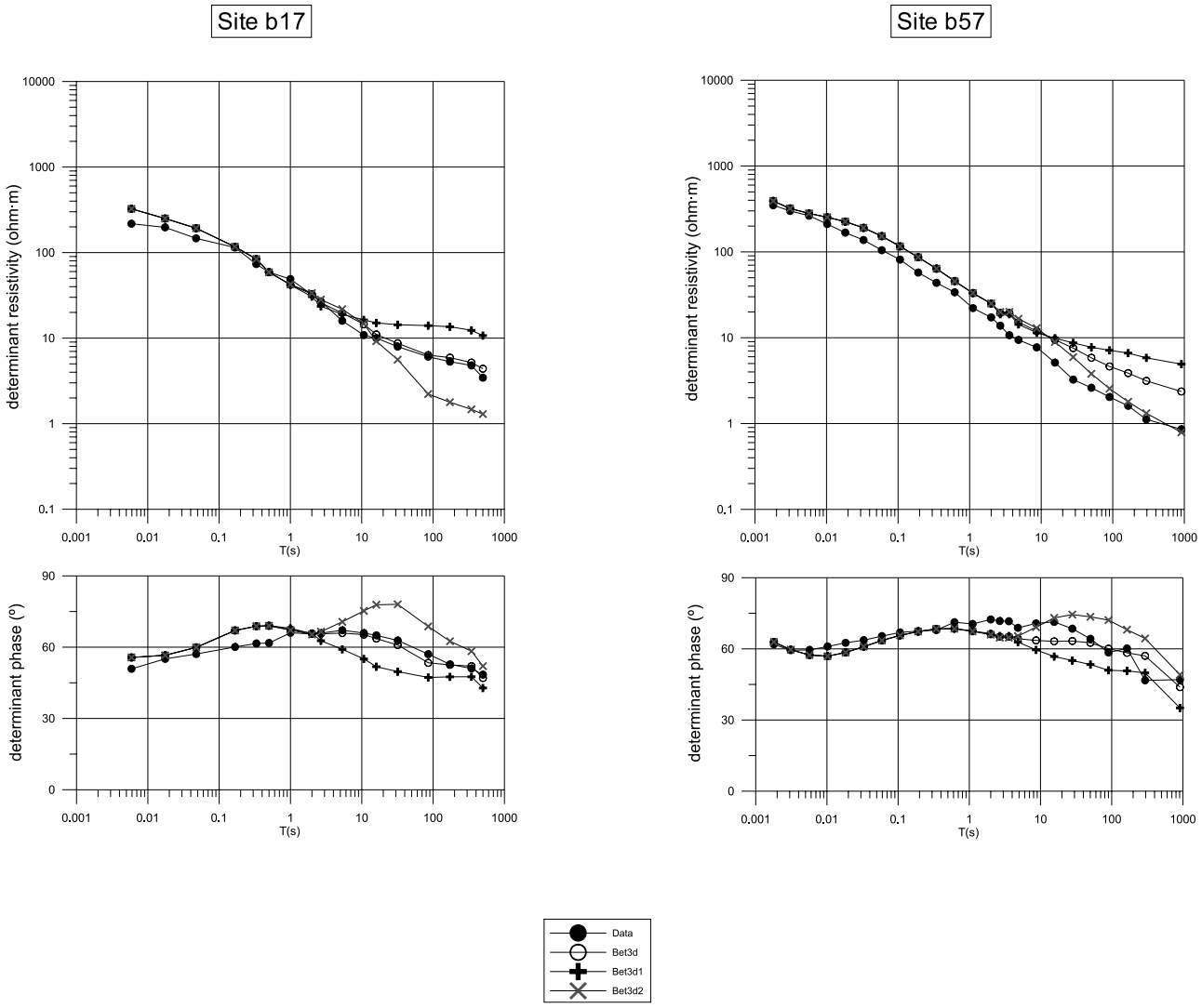

Figure 7. Determinant responses of data and models bet3d, bet3d1, and bet3d2 for sites 17 and 57, representative of the sites located over the conductive body CF3.

partial melt. However, the use of a larger data set and 3D techniques, proposed by *Ledo et al.* [2002], has allowed us to refine and redefine its depth, location and geometry, leading to an interpretation different from the previous work. This **CF3** conductor appears as a 7000 km^3 body placed at significantly shallower depths (between 4 km and 17.5 km) with a 90 km WNW-ESE extension. It is bounded at its base by a south dipping surface (see Figures 8 and 9) that coincides with the southern continuation of the sole thrust of the External Zone. This places the conductor in the core of the main antiform of the Sierra de los Filabres just above the major south dipping sole thrust. This separates the allochthonous rocks of the Alboran Domain from the autochthonous Iberian plate, allowing a new interpretation with important tectonic and geodynamic consequences.

5. Interpretation of the Conductive Body CF3 and Geodynamic Implications

[27] The extension and depth of conductor **CF3** (Figure 8) demonstrate that it belongs to the Alboran Domain, as opposed to the underlying Iberian crust (Figure 9). Its low resistivity can be explained by the presence of fluids, partial melting or a conducting mineral phase [e.g., *Jones*, 1992; *Nover*, 2005]. These possibilities have been investigated with other geophysical data. Anomaly **CF3** is located in a zone of low seismic activity, relatively high

Table 1. RMS Values of the Determinant, *xy* and *yx* Resistivity, and Phase Between Data and Model Responses for Model bet3d and the Two Models With Modifications in the Vertical Extent and Resistivity of the Conductive Body CF3: bet3d1 and bet3d2

Model	bet3D (Original)	bet3D1 (Higher Resistivity and Thickness)	bet3D2 (Lower Resistivity and Thickness)
RMS(ρ_{DET})	4.10	5.72	4.90
RMS (φ_{DET})	2.32	2.36	2.40
RMS(ρ_{xy})	7.53	8.29	7.54
RMS (φ_{xy})	3.69	3.70	3.72
RMS(ρ_{yx})	11.15	13.85	9.54
RMS (φ_{yx})	3.99	4.11	3.97

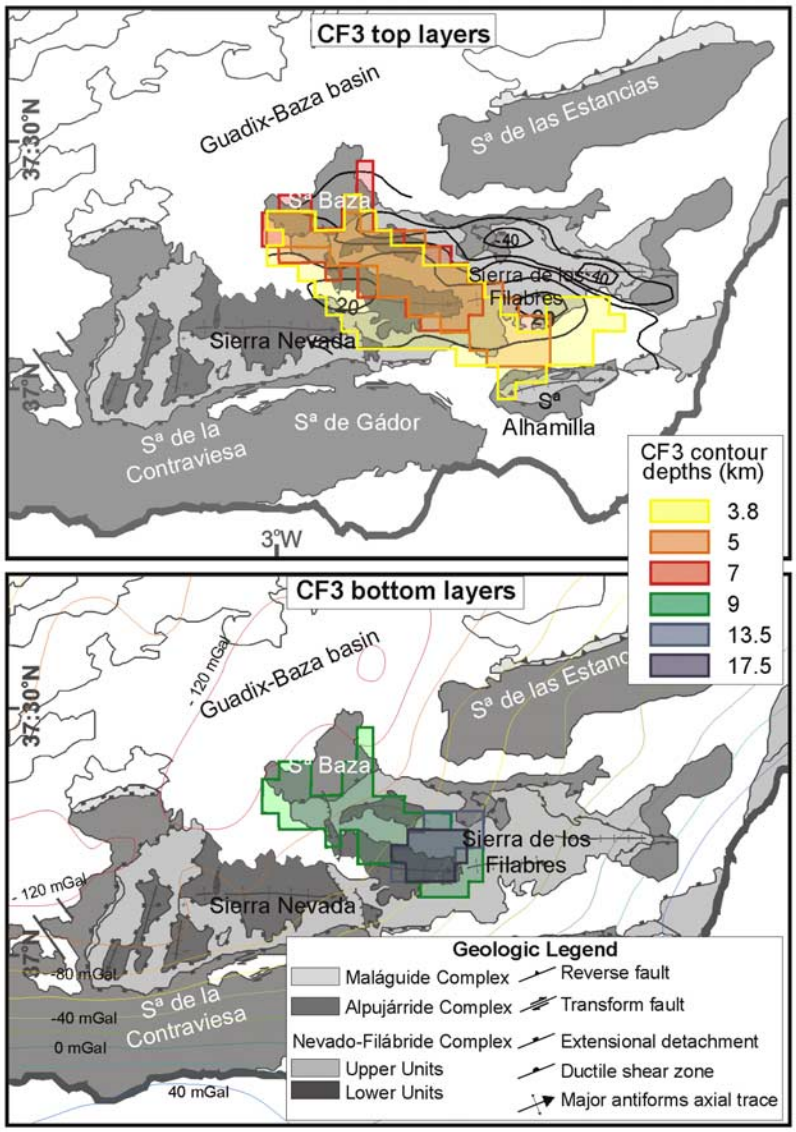

Figure 8. Geologic map of the central Internal Betics and contours of the top and bottom of CF3. (top) Solid lines indicate the location of the maximum and minimum of the magnetic anomaly. (bottom) Colored lines represent the Bouguer gravity anomaly map at 10-mGal interval.

seismic P velocity values [*Dañobeitia et al.*, 1998] and normal heat flow [*Fernàndez et al.*, 1998]. In addition, the topography of the area is uncorrelated with gravity data. That is, the maximum altitudes of the Betics do not coincide with a minimum in the Bouguer anomaly (Figure 8, bottom), where a crustal root should be observed [*Torné and Banda*, 1992]. These features suggest the presence of crustal detachment levels separating the uppermost crust formed by Alboran Domain rocks and subsequently deformed by large folds, from the Iberian Massif in its footwall [*Galindo-Zaldívar et al.*, 1997; *Marín-Lechado et al.*, 2007].

[28] Furthermore, there is a magnetic anomaly (−40 nT to +30 nT) with an almost E-W orientation, with the center of its western edge coinciding with the WNW edge of conductor **CF3** (Figure 8, top). This anomaly has been modeled as a 10-km-thick magnetic body caused by Fe mineralization along joints in the Nevado-Filábride metamorphic rocks, up to a depth of 10 km [*Galindo-Zaldívar et al.*, 1997]. Although this anomaly is not located precisely at the position of conductor **CF3**, it could be caused by a body with similar origin and composition.

[29] The emplacement of a dense body in the crust below the high peaks of Sierra Nevada and Sierra de los Filabres, and the addition of a crustal root, is compatible with the observed gravity data (e.g., a body with a density 0.1 g/cm^3 higher than the average crustal value will result in a crustal root of 7 km). Hence the conductive body **CF3** can have higher density than the average crustal rocks, which would allow for the existence of a crustal root below the Internal Zone.

[30] The presence of fluids alone makes it difficult to explain the large volume of the conductor, the moderately high seismic velocity values and its location just along the antiform crest. Moreover, in this case a continuous recharge mechanism would be necessary to ensure gravitational stability, for which there is no evidence. Within the fluids

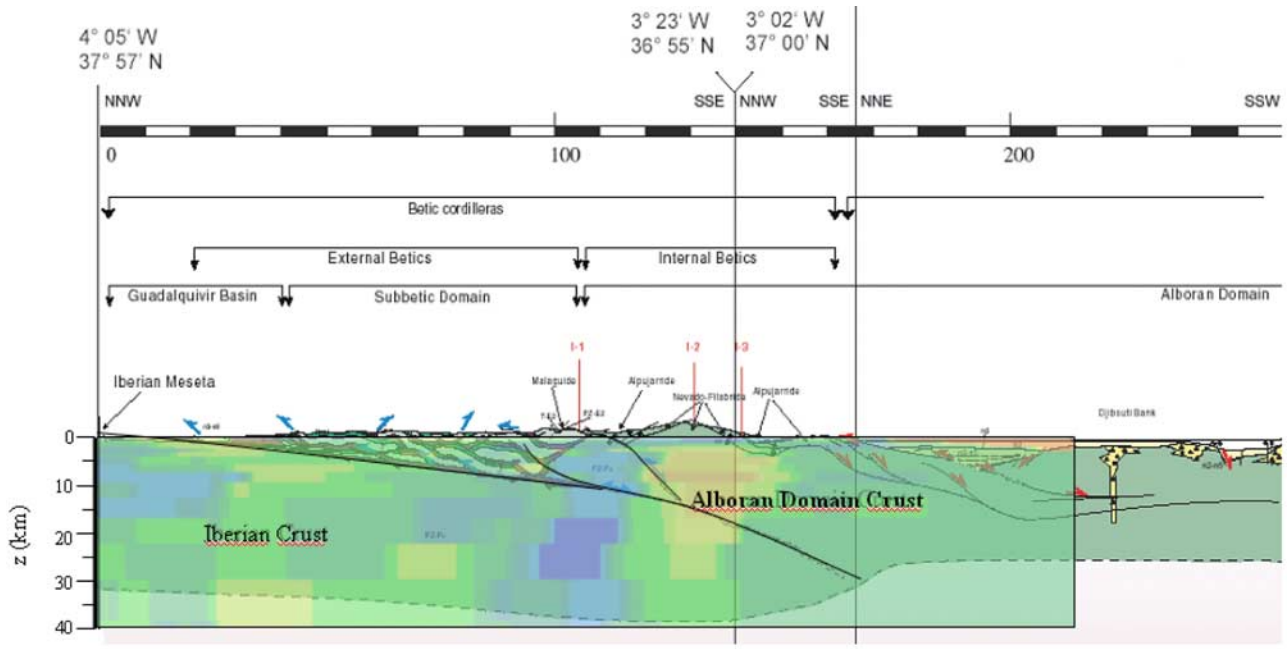

Figure 9. Transmed Transect I [*Frizon de Lamotte et al.*, 2004] with a NNW parallel cross section of the 3D conductivity model, cutting the conductor CF3.

hypothesis, anomaly **CF3** could specifically be some type of sediments associated with accreted oceanic crust (whose conductivity would be enhanced by the presence of water) [e.g., *Wu et al.*, 2005], but this would not be consistent with the high seismic velocities recorded. The partial melt hypothesis is improbable too, given that the temperatures suggested from heat flow data (between 325°C and 500°C) are not high enough [*Zappone et al.*, 2000]. Therefore the low resistivity of anomaly **CF3** is, most likely and plausibly, associated with a conducting mineral phase, a hypothesis that must be examined in more detail: What are the origins of this mineralization? Is it compatible with the present geodynamic models or does it imply proposing an alternative one?

[31] According to the geophysical observations, the conductor might also be a material with moderately high P velocity values, likely high density and could probably have high magnetic susceptibility (e.g., rocks containing massive sulfides or iron oxides [*Duba et al.*, 1994]). Although collocated geophysical observations are not necessarily linked to the same geologic feature [*Cook and Jones*, 1995], all these observations are compatible with one another. This higher density body would require a new gravity model, which could include the presence of a crustal root below the Internal Zone.

[32] Considering high seismic velocities and high density, the rocks hosting these conducting minerals must be ultrabasic or basic rocks, such as ophiolites or peridotites. In the Betics, rocks of the same type have been observed in small outcrops in the Nevado-Filábride complex (Cerro del Almirez [*López Sánchez-Vizcaíno et al.*, 2001]), and in widespread outcrops at the western sector of the Betics (Ronda [*Tubía et al.*, 1997]) and in the Rif Mountains [*Reuber et al.*, 1982]. Another possibility is that these hosting rocks are continental lower crustal rocks (amphibolites or granulites) that reached the upper crust during thrusting, deduced from the high metamorphic degree observed in rocks at the surface of the Internal Betics.

[33] An independent study that confirms the presence of conducting minerals in ultrabasic or basic rocks in the area has been presented by *Crespo et al.* [2006]. They describe graphite-sulfide deposits in the ultramafic rocks of Ronda and Beni-Bousera massifs, and use carbon isotope data to unravel the origin of carbon in mantle-derived rocks. The primary mineral assemblage of these deposits consists mainly of Fe-Ni-Cu sulfides (pyrrhotite, pentlandite, chalcopyrite and cubanite), graphite and chromite. These deposits were formed from residual melts that resulted from partial melting (and melt-rock reactions) of peridotites and pyroxenites by asthenospheric derived melts. These ultramafic massifs were emplaced in the lower crust 22 Ma ago, after undergoing partial melting and infiltration of asthenospheric melts resulting in the development of a recrystallization front [*Lenoir et al.*, 2001]. This evidence allows us to corroborate the hypothesis of the basic or ultrabasic rocks, as opposed to lower crustal rocks for which no evidence of conductive mineralizations has been found, as the most plausible to host the **CF3** conductor. The identification of such a body agrees with other authors [e.g., *Tubía et al.*, 1997] who state that the mechanism that emplaced basic or ultrabasic rocks (i.e., Ronda peridotites) not only affected the westernmost and southern parts of the Gibraltar Arc (Figure 1) but also its northern branch.

[34] Our interpretation requires reconsideration of most of the geodynamic models proposed for peridotite emplacement or Betics evolution because it substantially enlarges the area affected by this process and/or implies that, previous to the Betic orogeny, a thinned (oceanic?) lithospheric block existed between Iberia and the Alboran Domain. Additionally, the presence of a differentiated lithologic unit in the core of the main Nevado-Filábride antiform reinforces the hypothesis that the Internal Betics

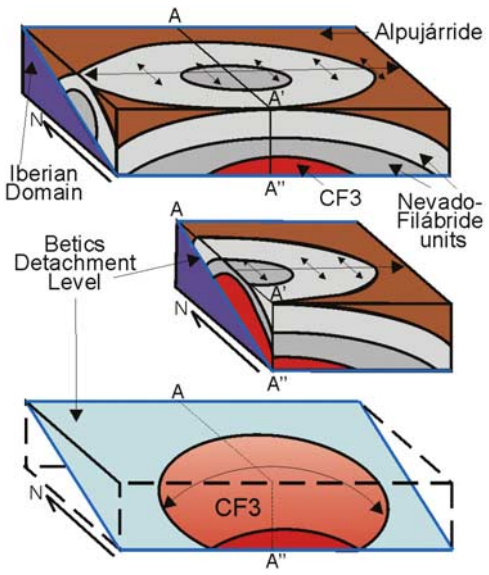

Figure 10. Schematic representation of CF3 in the core of the Sierra de Los Filabres antiform (Internal Zone).

are formed by an antiformal stack of crustal or even mantle thrust sheets [e.g., *Azañón et al.*, 2002], bounded below by the major south dipping sole thrust separating the Alboran Domain from Iberia (Figure 10).

[35] Taking into account the implicit piggyback sequence of thrust emplacement in the development of an antiformal stack, the structural location of the conductive body in the core of Nevado-Filábride implies that, previous to its emplacement, this new interpreted basic or ultrabasic unit was located in a more foreland position than the overlying Nevado-Filábride and Alpujárride blocks. This confirms that the preorogenic thinned (oceanic?) lithospheric block imaged by the conductive basic to ultrabasic body was located between Iberia and the Nevado-Filábride complex. The presence of this block in this particular structural position is not considered in the most recent work [e.g., *Gutscher et al.*, 2002; *Platt et al.*, 2006] and it entails reconsideration of the existing evolution models of the Betics. In particular, the structural position of the newly described basic to ultrabasic body beneath the Nevado-Filábride complex, as well as the presence of outcropping thrust slices of peridotites in the Alpujárride complex enables two different preorogenic geodynamic scenarios that explain the present contractional structure of the Internal Zone of the Betics (Figure 11.1).

[36] A. The first scenario proposes the existence of two well-differentiated oceanic lithospheric blocks, one located between the Nevado-Filábride complex and Iberia and another in a more hinterland position in the Alboran Domain (Figure 11.2-A). The first block would be defined by the **CF3** body and the second by the ensemble of Ronda

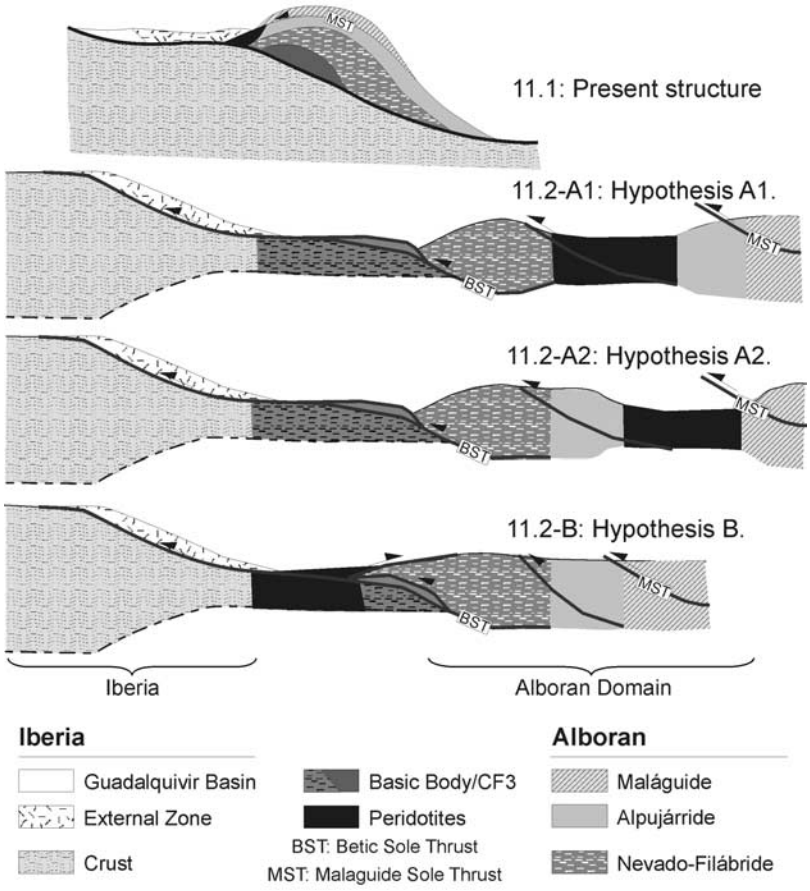

Figure 11. Sketches of the evolution hypotheses for the Betics related to the emplacement of major basic bodies evidencing sutures. 11.1, present structure; 11.2-A, hypotheses A1 and A2; 11.2-B, hypothesis B. Note that the sketches are representations of 3D processes, not 2D transects.

and Beni-Boussera peridotites, which could be located either between Nevado-Filábride and Alpujárride nappes (Figure 11.2-A1) or between Alpujárride and Maláguide [*Tubía et al.*, 1993] (Figure 11.2-A2). In this scenario, the present-day different structural position occupied by these bodies does not imply complex thrust kinematics. Instead, it suggests a simple piggyback stacking of thrust units originally placed in well differentiated continental or oceanic domains.

[37] B. The second scenario postulates the existence of only one suture between Iberia and Nevado-Filábride (Figure 11.2-B), being the common place of origin of both anomaly **CF3** and Ronda-Beni-Boussera peridotites. The present-day different structural position occupied by these bodies in the Internal Zone buildup is the result of the kinematics of thrust emplacement during the latest Cretaceous-Paleogene subduction and subsequent collision between Iberia and the Alboran Domain. In this scenario, the Ronda-Beni-Boussera peridotites are a series of ''oceanic'' thrust mantle slices of the subducting plate emplaced as back thrusts over the overriding taper in the last stages of thrust stacking. The conductive body **CF3** is a thrust sheet coming from the same subducting ''ocean'' but emplaced at the bottom of the same taper as a horst.

[38] Presently available data seem compatible with both scenarios that account for the presence of the electrical conductor at the innermost part of the Nevado-Filábride antiform. However, the first scenario (A1 or A2) is more compatible with models based on other data. Indeed, geochronologic and thermobarometric data [*Platt et al.*, 2006] also imply the existence of a suture between the Nevado-Filábride and Alpujárride-Maláguide complexes (model A1), whereas *Tubía et al.* [1993], based on structural and kinematic data, place the Ronda peridotites between the Alpujárride and Maláguide complexes (model A2).

6. Conclusions

[39] Using 3D MT techniques, a resistivity model of the central Betics crust has been constructed inferring a conductive body at upper-middle crustal levels in the Internal Zone. This body has been interpreted as a differentiated lithologic unit, probably made up of basic rocks, between the outcropping Nevado-Filábride complex and the Betic detachment level. We conclude that its conductivity is enhanced by the presence of a conducting mineral phase. The nature and location of this body has allowed us to construct two possible schemes for the evolution of the Betics and the emplacement of peridotitic bodies in the Gibraltar arc, which include two oceanic sutures or a single suture, respectively, within the Iberia and Alboran domains. The first one is thought to be the most suitable, given its compatibility with available data and other models proposed based on surface geological data.

[40] There are a large number of mountain belts formed as a collision of plates with remnant sutures (e.g., Alps, Himalayas). This paper shows how magnetotelluric studies can be a key tool to clarify what is the present position of the bodies implied in these sutures and the tectonic evolution responsible for their emplacement.

[41] **Acknowledgments.** The authors would like to thank Alex Marcuello and Claudia Arango from the University of Barcelona and Francisco González-Lodeiro, Fernando Bohoyo, Carlos Marín, Antonio Pedrera, Vicente Pérez, Patricia Ruano y Ana Ruiz, from the Departamento de Geodinámica of the University of Granada for their valuable help in the field data acquisition. This paper has been improved by the very useful comments of Alan G. Jones, Paul A. Bedrosian, Ian Ferguson, an anonymous reviewer, associate editor Domenico Patella, and editor Richard Arculus. This work was supported by projects CGL2006-10166, CGL2006-06001, and CGL2007-66431-C02-01/BTE from the Ministerio de Educación y Ciencia of Spain.

References

Azañón, J. M., J. Galindo-Zaldívar, V. García-Dueñas, and A. Jabaloy (2002), Alpine tectonics. II: Betic Cordillera and Balearic Islands, in *The Geology of Spain*, edited by W. Gibbons and T. Moreno, pp. 401–416, Geol. Soc., London, U.K.

Balanyá, J. C., and V. García-Dueñas (1987), Les directions structurales dans le Domaine d'Alboran de part et d'autre du Detroit de Gibraltar, *C. R. Acad. Sci. Paris*, *304*, 929–932.

Constable, S. C., R. L. Parker, and C. G. Constable (1987), Occam's inversion: A practical algorithm for generating smooth models from EM sounding data, *Geophysics*, *63*, 816–825.

Cook, F. A., and A. G. Jones (1995), Seismic reflections and electrical conductivity: A case of Holmes's curious dog?, *Geology*, *23*, 141–144.

Crespo, E., F. J. Luque, M. Rodas, H. Wada, and F. Gervilla (2006), Graphite-sulfide deposits in Ronda and Beni Bousera peridotites (Spain and Morocco) and the origin of carbon in mantle-derived rocks, *Gondwana Res.*, *9*, 279–290.

Dañobeitia, J. J., V. Sallarès, and J. Gallart (1998), Local earthquakes seismic tomography in the Betic Cordillera (southern Spain), *Earth Planet. Sci. Lett.*, *160*, 225–239.

DeGroot-Hedlin, C., and S. Constable (1993), Occam's inversion and the North American central plains electrical anomaly, *J. Geomagn. Geoelectr.*, *45*, 985–999.

Doglioni, C., M. Fernàndez, E. Gueguen, and F. Sabat (1999), On the interference between the early Apennines-Maghrebides backarc extension and the Alps-Betics orogen in the Neogene geodynamics of the western Mediterranean, *Bolletin Soc. Geol. Ital.*, *118*, 75–89.

Duba, A., S. Heikamp, W. Meurer, G. Nover, and G. Will (1994), Evidence from borehole samples for the role for accessory minerals in lower-crustal conductivity, *Nature*, *367*, 59–61.

Egbert, G. D., and J. R. Booker (1986), Robust estimation of geomagnetic transfer functions, *Geophys. J. R. Astron. Soc.*, *87*, 173–194.

Fernàndez, M., I. Marzán, A. Correia, and E. Ramalho (1998), Heat flow, heat production, and lithospheric thermal regime in the Iberian Peninsula, *Tectonophysics*, *291*, 29–54.

Frizon de Lamotte, D., et al. (2004), TRANSMED Transect I, in *The TRANSMED Atlas - The Mediterranean Region From Crust to Mantle* [CD-ROM], edited by W. Cavazza et al., Springer, Berlin.

Gabàs, A., and A. Marcuello (2003), The relative influence of different types of magnetotelluric data on joint inversions, *Earth Planets Space*, *55*, 243–248.

Galindo-Zaldívar, J., A. Jabaloy, F. González-Lodeiro, and F. Aldaya (1997), Crustal structure of the central sector of the Betic Cordillera (SE Spain), *Tectonics*, *16*, 18–37.

García-Dueñas, V., J. C. Balanyá, and J. J. Martínez-Martínez (1992), Miocene extensional detachment in the outcropping basement of the northern Alboran basin (Betics) and their tectonic implications, *Geo-Mar. Lett.*, *12*, 88–95.

García-Dueñas, V., E. Banda, M. Torné, D. Córdoba, and ESCI-Béticas Working Group (1994), A deep seismic reflection survey across the Betic chain (southern Spain): First results, *Tectonophysics*, *232*, 77–89.

García-Hernández, M., A. C. López-Garrido, P. Rivas, C. Sanz de Galdeano, and J. Vera (1980), Mesozoic paleogeographic evolution in the External Zones of the Betic Cordillera (Spain), *Geol. Mijnbouw*, *59*, 155–168.

Groom, R. W., and R. C. Bailey (1989), Decomposition of the magnetotelluric impedance tensor in the presence of local three-dimensional galvanic distortion, *J. Geophys. Res.*, *94*, 1913–1925.

Gutscher, M. A., J. Malod, J. P. Rehault, I. Contrucci, F. Klingelhoefer, L. Mendes-Victor, and W. Spakman (2002), Evidence for active subduction beneath Gibraltar, *Geology*, *30*, 1071–1074.

Heise, W., T. G. Caldwell, H. M. Bibby, and S. C. Bannister (2008), Three-dimensional modelling of magnetotelluric data from the Rotokawa geothermal field, Taupo Volcanic Zone, New Zealand, *Geophys. J. Int.*, *173*, 740–750.

Jolivet, L., and C. Faccenna (2000), Mediterranean extension and the Africa-Eurasia collision, *Tectonics*, *19*, 1095–1106.

Jones, A. G. (1992), Electrical conductivity of the continental lower crust, in *Continental Lower Crust*, edited by D. M. Fountain, R. J. Arculus, and R. W. Kay, pp. 81–143, Elsevier, New York.

Jones, A. G. (1993), The COPROD2 dataset: Tectonic setting, recorded MT data and comparison of models, *J. Geomagn. Geoelectr.*, *45*, 933–955.

Jones, A. G., P. Lezaeta, I. J. Ferguson, A. D. Chave, R. L. Evans, X. Garcia, and J. Spratt (2003), The electrical structure of the Slave craton, *Lithos*, *71*, 505–527.

Korja, T. (2007), How is the European lithosphere imaged by magnetotellurics?, *Surv. Geophys.*, *28*, 239–272.

Ledo, J., C. Ayala, J. Pous, P. Queralt, R. W. Marcuello, and J. A. Muñoz (2000), New geophysical constraints on the deep structure of the Pyrenees, *Geophys. Res. Lett.*, *27*, 1037–1040.

Ledo, J., P. Queralt, A. Martí, and A. G. Jones (2002), Two-dimensional interpretation of three-dimensional magnetotelluric data: An example of limitations and resolution, *Geophys. J. Int.*, *150*, 127–139.

Lenoir, X., C. J. Garrido, J. L. Bodinier, J. M. Dautria, and F. Gervilla (2001), The recrystallization front of the Ronda peridotite: Evidence for melting and thermal erosion of subcontinental lithospheric mantle beneath the Alboran basin, *J. Petrol.*, *42*, 141–158.

López Sánchez-Vizcaíno, V., D. Rubatto, M. T. Gómez-Pugnaire, V. Trommsdorff, and O. Müntener (2001), Middle Miocene high-pressure metamorphism and fast exhumation of the Nevado-Filábride Complex, SE Spain, *Terra Nova*, *13*, 327–332.

Mackie, R. L., T. R. Madden, and P. E. Wannamaker (1993), Three-dimensional magnetotelluric modeling using difference equations—Theory and comparisons to integral equation solutions, *Geophysics*, *58*, 215–226.

Marín-Lechado, C., J. Galindo-Zaldívar, L. R. Rodriguez-Fernández, and A. Pedrera (2007), Mountain front development by folding and crustal thickening in the internal zone of the Betic Cordillera-Alboran Sea boundary, *Pure Appl. Geophys.*, *164*, 1–21.

Martí, A. (2006), A magnetotelluric investigation of geoelectric dimensionality and study of the Central Betic crustal structure, Ph.D. thesis, Univ. of Barcelona, Barcelona, Spain.

Martí, A., P. Queralt, and E. Roca (2004), Geoelectric dimensionality in complex geological areas: Application to the Spanish Betic Chain, *Geophys. J. Int.*, *157*, 961–974.

McNeice, G., and A. G. Jones (2001), Multisite, multifrequency tensor decomposition of magnetotelluric data, *Geophysics*, *66*, 158–173.

Nover, G. (2005), Electrical properties of crustal and mantle rocks—A review of laboratory measurements and their explanation, *Surv. Geophys.*, *26*, 593–651.

Pedersen, L. B., and M. Engels (2005), Routine 2D inversion of magnetotelluric data using the determinant of the impedance tensor, *Geophysics*, *70*, G33–G41.

Platt, J. P., and R. L. M. Vissers (1989), Extensional collapse of thickened continental lithosphere: A working hypothesis for the Alboran Sea and the Gibraltar arc, *Geology*, *17*, 540–543.

Platt, J. P., R. Anczkiewicz, J. I. Soto, S. P. Kelley, and M. Thirlwall (2006), Early Miocene continental subduction and rapid exhumation in the western Mediterranean, *Geology*, *34*, 981–984.

Pous, J., P. Queralt, J. J. Ledo, and E. Roca (1999), A high electrical conductive zone at lower crustal depth beneath the Betic Chain (Spain), *Earth Planet. Sci. Lett.*, *167*, 35–45.

Pous, J., P. Queralt, and A. Marcuello (2001), Magnetotelluric signature of the western Cantabrian Mountains, *Geophys. Res. Lett.*, *28*, 1795–1798.

Rao, C. K., A. G. Jones, and M. Moorkamp (2007), The geometry of the Iapetus Suture Zone in central Ireland deduced from a magnetotelluric study, *Phys. Earth Planet. Inter.*, *161*, 134–141.

Reuber, I., A. Michard, A. Chalouan, T. Juteau, and B. Jermoumi (1982), Structure and emplacement of the Alpine-type peridotites from Beni Bousera, Rif, Morocco: A polyphase tectonic interpretation, *Tectonophysics*, *82*, 231–251.

Seber, D., M. Barazangi, A. Ibenbrahim, and A. Demnati (1996), Geophysical evidence for lithospheric delamination beneath the Alboran Sea and Rif-Betics mountains, *Nature*, *379*, 785–790.

Serrano, I., J. Morales, D. Zhao, F. Torcal, and F. Vidal (1998), P-wave tomographic images in the Central Betics-Alborán Sea (south Spain) using local earthquakes: Contribution for a continental collision, *Geophys. Res. Lett.*, *25*, 4031–4034.

Tauber, S., R. Banks, O. Ritter, and U. Weckmann (2003), A high-resolution magnetotelluric survey of the Iapetus Suture Zone in southwest Scotland, *Geophys. J. Int.*, *153*, 548–568.

Torné, M., and E. Banda (1992), Crustal thinning from the Betic Cordillera to the Alboran Sea, *Geo-Mar. Lett.*, *12*, 76–81.

Tubía, J. M., F. Navarro-Vilá, and J. Cuevas (1993), The Maláguide-Los Reales Nappe: An example of crustal thinning related to the emplacement of the Ronda peridotites (Betic Cordillera), *Phys. Earth Planet. Inter.*, *78*, 343–354.

Tubía, J. M., J. Cuevas, and J. I. Gil-Ibarguchi (1997), Sequential developments of the metamorphic aureole beneath the Ronda peridotites and its bearing on the tectonic evolution of the Betic Cordillera, *Tectonophysics*, *279*, 227–252.

Unsworth, M. J., A. G. Jones, W. Wei, G. Marquis, S. G. Gokarn, J. E. Spratt, and INDEPTH-MT Team (2005), Crustal rheology of the Himalaya and southern Tibet inferred from magnetotelluric data, *Nature*, *438*, 78–81.

Weaver, J. T., A. K. Agarwal, and F. E. M. Lilley (2000), Characterisation of the magnetotelluric tensor in terms of its invariants, *Geophys. J. Int.*, *141*, 321–336.

Wu, X., I. J. Ferguson, and A. G. Jones (2005), Geoelectric structure of the Proterozoic Wopmay Orogen and adjacent terranes, Northwest Territories, Canada, *Can. J. Earth Sci.*, *42*, 955–981.

Zappone, A., M. Fernàndez, V. García-Dueñas, and L. Burlini (2000), Laboratory measurements of seismic *P*-wave velocities on rocks from the Betic chain (southern Iberian Peninsula), *Tectonophysics*, *317*, 259–272.

J. Galindo-Zaldívar, Instituto Andaluz de Ciencias de la Tierra y Departamento de Geodinámica, Universidad de Granada, Campus Fuentenueva, s/n, E-18002 Granada, Spain.

J. Ledo, A. Martí, P. Queralt, and E. Roca, Departament de Geodinàmica i Geofísica, Universitat de Barcelona, Martí i Franquès, s/n, E-08028 Barcelona, Spain. (annamarti@ub.edu)